CBPF-NF-042/98

Quantum Section Method for the Soft Stadium

by

J.S.Espinoza Ortiz and A.M. Ozorio de Almeida

Centro Brasileiro de Pesquisas Físicas - CBPF
Rua Dr. Xavier Sigaud, 150
22290-180 – Rio de Janeiro, RJ – Brazil

Abstract

The Soft Stadium is defined by a monomial potential with exponent 2α as a parameter, such that $\alpha \to \infty$ correspond to the billard. The practical use of the quantum section method depends only the partial separability of the system on both sides of a section. This is possible for all α's. In particular, for $\alpha = 1$, the system becomes globally separable, allowing for a general test of the method. We also tested the use of the asymptotic W.K.B. type approximation for higher energy eigenvalues. We show that all these alternative methods are in excelent agreement.

Key-words: Quantum section, Soft Stadium, Asymptotic W.K.B. theory.

Introduction

The section method was originally divised by Bogomolny as a basis for the resummation of periodic orbits contributing to the energy spectrum of chaotic systems in the semiclassical approximation[1]. However, this approximation was later formally derived from fully quantum mechanical Green functions, leading in principle to exact eigenvalue conditions[2]. These were explicitly developed for separable systems [3] and for a particular chaotic system, the quarter-stadium[4].

The possibility for direct construction of the Green function on both sides of the section in [4] depends on the property of partial separability of the quarter stadium. This is not restricted to billards; indeed, the Hamiltonian system

$$\mathcal{H} = \frac{1}{2}p_x^2 + \frac{1}{2}p_y^2 + V(x,y), \tag{1}$$

with the potential given by

$$V(x,y) = \begin{cases} \frac{1}{2}\left(\sqrt{x^2+y^2}\right)^{2\alpha} & ;x,y \geq 0\,, \\ \frac{1}{2}y^{2\alpha} & ;y \geq 0,\ x \in (-b,0)\,, \\ \infty & ;\text{at } x=-b \text{ and } y=0\,, \end{cases} \tag{2}$$

(where α, b are real positive parameters), converges onto the quarter-stadium billard, but it is separable on both sides of the section $x = 0$. The section method is extremely economical, depending on a determinant that grows only with the square root of the energy. This is useful even for billards (for wich many special methods are available:[5],[6],[7]), but for 'soft' Hamiltonian systems, this is an enormous advantage. The case of the quarter-stadium is specially interesting, because it is the basis for the description of experiments with the conductivity of quantum dots([8],[9],[10]), wich are assumed to be hard billards just to simplify analysis.

In this paper we will set up an eigenvalue condition within the section method for the particular case where the parameter $\alpha = 1$. This is easily generalized for $\alpha > 1$, while permitting an exact test for the method since the system is then separable without any reference to the section. We can then also test the use of the asymptotic W.K.B. type approximation in the construction of the Green functions, allowing us to easily acces higher energy eigenvalues. This is important since, so far, we have only compared the method with alternative numerical approximations[4].

In section 1 we summarize the dynamics of this system and construct its Poincaré map. In section 2 , the first two kinds of solutions are presented while the asymptotic W.K.B. type approximation is presented in section 3. Non-oscillating mode contributions to spectra are discussed in section 4. To verify spectral completeness we calculated the mean cumulative density of states in section 5. Results and a brief discussion are presented in section 6 .

1 The Classical Poincaré section

The dynamics of the Hamiltonian (1) with potential given by (2) for the particular parameter $\alpha = 1$ can be more easily described when considering the Poincaré section 'Σ'

exactly at $x = 0$. This plane separates the potential with radial symmetry (region I) from the potential with planar symmetry (region II), figure 1. Setting the first point $Q\prime$ on the section, the Poincaré map considers the trajectory into some point $Q\prime\prime$ on the section itself after visiting once both regions I and II, respectively. Sucessive traversals of the points $Q\prime$ and $Q\prime\prime$ with respective momenta $P\prime$ and $P\prime\prime$ generates the map [11].

It is important to note that in region I the equation of motion for the x and y modes are given by the harmonic oscilator equation with the same period π . The orbits are periodic, so a trajectory going out from a point on the section comes back into itself. We see that the dynamics in region I will not influence the dynamics in region II.

Now we consider dynamics in region II. In the x mode, the momentum is constant while, for the y mode, the dynamics are given by the harmonic oscillator equation with period π . Note that the time spent by a trajectory that starts at the plane $x = 0$ and comes back into itself, after reflecting with the plane $x = -b$, depends on the x-mode and it is given by $t_x = \frac{2b}{p_x}$. It is interesting to note that we can describe all possible trajectories by fixing the parameter b and by changing p_x so the time t_x could be written in a general form as $t_x = m\pi + \delta\, t$ (with m integer and $\delta\, t$ real). Note that, choosing $\delta\, t$ as a rational part of π, we obtain closed trajectories; the map $(p_y \times y)$ becomes a finite seqüence of fixed points located on the circle $\left(p_y^2 + y^2 = k^2 - p_x^2\right)$. When $\delta\, t$ is an irrational the orbits are not closed and the points on the circle become dense. Some orbits described here are shown in figure 2.

The complete set of soft stadia from $\alpha = 1$ to $\alpha \to \infty$ span all the examples from fully integrable motion to hard chaos.

2 The methods

We shall consider the Schrödinger equation for a particle with unitary mass.

2.1 First method

This method makes no reference to the section, because it is based on the separability of Schrödinger's equation in rectangular coordinates, for $\alpha = 1$.

For the Schrödinger equation in y coordinates we have

$$\left\{\frac{d^2}{dy^2} + \kappa_y^2 - y^2\right\}\psi_{1,2}(y) = 0 \quad ; y \geq 0 \ , \tag{3}$$

and in x coordinates

$$\begin{aligned} \left\{\frac{d^2}{dx^2} + \kappa^2 - \kappa_y^2\right\}\varphi_2(x) = 0 \quad & ; x \in (-b, 0), \\ \left\{\frac{d^2}{dx^2} + \kappa^2 - \kappa_y^2 - x^2\right\}\varphi_1(x) = 0 \quad & ; x \geq 0, \end{aligned} \tag{4}$$

where $\kappa^2 = 2E$, with E as energy parameter.

Equation (3) is easily solved [12],

$$\psi_{1,2}^n(y) = e^{-\frac{1}{2}y^2} H_{2n-1}(y); \quad n \geq 1, \text{ integer.} \tag{5}$$

Here $H_{2n-1}(y)$ are the odd Hermite polinomials, because we are imposing $\psi(0) = 0$. Replacing $\kappa_y^2 = 4n - 1$ and defining $\kappa_n^2 = \kappa^2 - \kappa_y^2$ in equation (4) we obtain

$$\begin{array}{ll} \varphi_2(x;\kappa_n) \propto \sin\kappa_n(x+b) & ;x \in (-b,0)\,, \\ \varphi_1(x;\kappa_n) \propto U\left(\frac{1}{2}\kappa_n^2, \sqrt{2}x\right) & ;x \geq 0\,. \end{array} \tag{6}$$

In (6), for the first solution we imposed $\psi(-b;\kappa_n) = 0$. The solutions for $x \geq 0$ are called parabolic cylinder functions[13], for which we imposed that in the limit $x \to \infty$ they decay as $e^{-\frac{1}{2}x^2}$.

Fixing the n eigenmode in y cordinates, eigenvalues are obtained matching the φ solutions at $x = 0$. This condition imposes that the Wronskian of both functions at $x = 0$ must be zero at the eigenvalue 'E_i'; i.e:

$$\mathcal{W}(E_i) = \left\{\varphi_1(x)\partial_x\varphi_2(x) - \varphi_2(x)\partial_x\varphi_1(x)\right\}|_{x=0} = 0\,. \tag{7}$$

2.2 Second method

This is based on the section, considering rectangular coordinates in region II of figure 1 and cylindrical coordinates in region I.

For region II we have

$$\begin{array}{ll} \Psi_2(x,y) & = \sum_n \alpha_n \psi_2^n(y)\varphi_2(x;\kappa_n), \\ & = \sum_{n\geq 1} \alpha_n \exp\left(-\frac{1}{2}y^2\right) H_{2n-1}(y)\frac{1}{\kappa_n}\sin\kappa_n(x+b);\ \alpha_n \neq 0,\in \Re. \end{array} \tag{8}$$

For region I, separating Schrödinger's equation in cylindrical coordinates, we have

$$\begin{array}{rl} \left\{\frac{d^2}{dr^2} + \frac{1}{r}\frac{d}{dr} + \kappa^2 - \frac{\nu^2}{r^2} - r^2\right\}\psi_1 & = 0\,, \\ \left\{\partial_\phi^2 + \nu^2\right\}\varphi_1 & = 0\,. \end{array} \tag{9}$$

Before solving the first equation above, it is important to note that in the limit $r \to \infty$ this equation behaves like an harmonic oscilator equation, and because of this behaviour we try $\psi_1(r) = e^{-\frac{1}{2}r^2}\chi(r)$. After replacing ψ_1 in the first equation (9), we obtain a new radial equation,

$$\left\{\frac{d^2}{dr^2} + \left(-2r + \frac{1}{r}\right)\frac{d}{dr} + \left(\kappa^2 - 2 - \frac{\nu^2}{r^2}\right)\right\}\chi(r) \quad = 0\,. \tag{10}$$

Solving (10) we obtain

$$\chi(r) \quad = r^\nu F\left(a;c;r^2\right) \quad ;a = \left(\tfrac{\nu+1}{2} + E\right) \text{ and } \ c = \nu + 1\,, \tag{11}$$

where $F\left(a;c;r^2\right)$ are the confluent hypergeometric functions[13].

But the χ polinomial converges to $e^{\frac{1}{2}r^2}$, so we have to cut the χ series and quantize the angular momenta, ie:

$$\nu(E) = E + 1 - 2m \quad ;m \geq 1\,. \tag{12}$$

From here we have that given E there will be m_{max} eigenmodes, given by the integer part of the real number $(E+1)/2$. In this way we arrived at the solution for $\psi_1^m(r)$, which we write as

$$\psi_1^m(r) \propto e^{-\frac{1}{2}r^2}\, r^{\nu_m} F\left(\frac{\nu_m+1}{2}+E;\nu_m+1;r^2\right) \ , \tag{13}$$

where $\nu_m = \nu_m(E)$, given by (12). It is interesting that in the limit $\nu_m \to 0$, $\psi_1^m(r)$ behaves like an harmonic oscillator function, otherwise it behaves like a Bessel function of real order. Finally, solving the angular equation, we obtain

$$\varphi_1(\phi,k) \propto \frac{1}{\nu_m}\sin\nu_m\left(\pi/2-\phi\right) \ . \tag{14}$$

Now we can construct

$$\begin{array}{ll} \Psi_1(\phi,r) & = \sum_m \beta_m \psi_1^m(r)\varphi_1(\phi,k)\,; \\ & = \sum_m \beta_m \exp\left(-r^2/2\right)\chi^{\nu_m}(r)\frac{1}{\nu_m}\sin\nu_m(\frac{\pi}{2}-\phi)\,;\beta_m \neq 0,\in \Re. \end{array} \tag{15}$$

Eigenvalues are found by establishing that on the section the integral Wronskian of functions $\Psi_{1,2}$ has to be zero at the eigenvalue 'E_i', that is,

$$\mathcal{W}(E_i) = \int_0^\infty dy\, \left\{\Psi_2(x,y)\partial_n\Psi_1(\phi,r) - \Psi_1(\phi,r)\partial_n\Psi_2(x,y)\right\}|_{(x,\phi=0);r=y} = 0\,. \tag{16}$$

Following[4] we can rewrite (16) as a matrix equation with real elements

$$\Pi_{nm}(E) = \frac{\sin k_n b}{k_n} < n|m > \cos\nu_m\frac{\pi}{2} + \cos k_n b < n|m >^{-1} \frac{\sin\nu_m\frac{\pi}{2}}{\nu_n}, \tag{17}$$

where the integrals calculated explicitly on the section are defined by :

$$\begin{array}{ll} < n|m > & = \int_0^\infty \frac{dy}{y}\psi_2^n(y)\psi_1^m(y)\,; \\ < n|m >^{-1} & = \int_0^\infty dy\,\psi_2^n(y)\psi_1^m(y)\,. \end{array} \tag{18}$$

The matching condition for eigenvalues 'E_i' then become

$$\det\Pi(E_i) = 0\,. \tag{19}$$

3 Asymptotic W.K.B. approximation

We approximate the eigenmodes using W.K.B. theory and solve the eigenvalue problem using equation (19). Given Schrödinger's equation (3) for the y coordinate in region II , it is well known that solutions can be approximated in the form[14]

$$\psi_2(y) \propto \left\{ \begin{array}{ll} \frac{2}{\sqrt[4]{\kappa_y^2-y^2}}\cos\left(s_<(y)-\frac{\pi}{4}\right) & ;0<y<\kappa_y\,, \\ \frac{1}{\sqrt[4]{y^2-\kappa_y^2}}\exp -s_>(y) & ;\ \kappa_y<y<\infty\,, \end{array} \right. \tag{20}$$

where we define

$$\begin{aligned} \mathrm{s}_<(y) &= \int_y^{\kappa_y} dy\sqrt{\kappa_y^2 - y^2}; \\ &= \left(\frac{\pi}{2} - \frac{y}{\kappa\, y}\sqrt{1-\frac{y^2}{\kappa_y^2}} - \arcsin\frac{y}{\kappa_y}\right)\kappa_y^2/2, \\ \mathrm{s}_>(y) &= \int_{\kappa_y}^{y} dy\sqrt{y^2 - \kappa_y^2}\,; \\ &= \frac{y}{2}\sqrt{y^2-\kappa_y^2} + \frac{\kappa_y^2}{2}\log\left(\frac{\kappa_y}{\sqrt{y^2-\kappa_y^2}+y}\right). \end{aligned} \tag{21}$$

Imposing the boundary condition for ψ_2, ie $\psi_2(0) = 0$, we obtain

$$\kappa_y^2 = 4n + 3, \quad n \geq 1, \tag{22}$$

by considering the first equation in (21).

Now, considering the problem in region I, given the Schrödinger equation in cylindrical coordinates (9), we make the substitution $\psi_1(r) = \frac{1}{\sqrt{r}}\zeta(r)$ and change $\nu^2 - 1/4 \to \nu^2$ [15], arriving at the equation

$$\left(\frac{d^2}{dr^2} + \kappa^2 - \frac{\nu^2}{r^2} - r^2\right)\zeta(r) = 0\,. \tag{23}$$

Here we just give the explicit radial function (leaving detailed development for appendix A).

$$\psi_1 = \begin{cases} \frac{2/\sqrt{r}}{\sqrt[4]{\frac{\nu^2}{\kappa^2}+r^2-\kappa^2}}\exp \mathrm{s}_<(r) & ;r < r_1\,, \\ (-1)^{m+1}\,\frac{2/\sqrt{r}}{\sqrt[4]{\kappa^2-\frac{\nu^2}{\kappa^2}-r^2}}\cos\left(\mathrm{s}_{1,2}(r) - \frac{\pi}{4}\right) & ;r_1 < r < r_2\,, \\ \frac{2/\sqrt{r}}{\sqrt[4]{\frac{\nu^2}{\kappa^2}+r^2-\kappa^2}}\exp -\mathrm{s}_>(r) & ;r > r_2\,, \end{cases} \tag{24}$$

where the turning points $r_{1,2} = \sqrt{\frac{1}{2}\left(\kappa^2 \pm \sqrt{\kappa^4 - 4\nu^2}\right)}$; $r_1 < r_2$. The actions are given by the expressions

$$\begin{aligned} \mathrm{s}_<(r) &= \tfrac{1}{2}\sqrt{\nu^2 + r^4 - \kappa^2 r^2} - \log\left\{\left(\frac{\frac{2\nu^2}{r^2}+\frac{2\nu}{r}\sqrt{\frac{\nu^2}{r^2}+r^2-\kappa^2}-\kappa^2}{\sqrt{\kappa^2-4\nu^2}}\right)^{\nu/2}\left(\frac{2r^2+2\sqrt{\nu^2+r^4-\kappa^2r^2}-\kappa^2}{\sqrt{\kappa^4-4\nu^2}}\right)^{\kappa^2/4}\right\} \\ \mathrm{s}_>(r) &= \tfrac{1}{2}\sqrt{\nu^2 + r^4 - \kappa^2 r^2} - \log\left\{\left(\frac{\kappa^2-\frac{2\nu^2}{r^2}-\frac{2\nu}{r}\sqrt{\frac{\nu^2}{r^2}+r^2-\kappa^2}}{\sqrt{\kappa^2-4\nu^2}}\right)^{\nu/2}\left(\frac{2r^2+2\sqrt{\nu^2+r^4-\kappa^2r^2}-\kappa^2}{\sqrt{\kappa^4-4\nu^2}}\right)^{\kappa^2/4}\right\} \\ \mathrm{s}_{1,2}(r) &= \left(\frac{\kappa^2}{2}-\nu\right)\frac{\pi}{4} - \frac{r}{2}\sqrt{\kappa^2-\frac{\nu^2}{r^2}-r^2} + \frac{\nu}{2}\arcsin\frac{\kappa^2-\frac{2\nu^2}{r^2}}{\sqrt{\kappa^4-4\nu^2}} + \frac{\kappa^2}{4}\arcsin\frac{\kappa^2-2r^2}{\sqrt{\kappa^4-4\nu^2}}\,, \end{aligned} \tag{25}$$

and the angular momenta $\nu = (E + 1 - 2m)\,; k \geq 1$.

The solutions (20) and (24) break down in the neighbourhood of the turning points, but they can be replaced by uniform approximations based on Airy functions[16].

4 Non-oscillating modes

There is no restriction for the number of eigenmodes to be considered in the solutions in the past sections. For $x \leq 0$ we see that when $k_y > \kappa$ the transverse wave number k_n become imaginary, that is, the corresponding mode will be of the form $\sinh k_n(x+b)$, a superposition of exponentially increasing and decreasing modes. Because the amplitude must remain finite, the weight of the non-oscillating modes will decrease rapidly with n.

For $x \geq 0$ we have to analize two situations. In the first method , when k_n is imaginary, the eigenmodes behave like $\exp(-|k_n|x)$ for $x < |k_n|$,(this corresponds to the asymptotic behaviour of hyperbolic cylinder functions[13]).

Now we will study the contributions from non-oscillating modes in the second method and its asymptotic approximation. To understand the behaviour of these eigenmodes it is better consider (23). To include non-oscillating modes in the transversal angular direction, the angular momenta ν must become imaginary and the singular potential for this Schrödinger equation becomes strongly attractive close to the origin. For this situation we see that ζ is strongly bounded , and oscillates increasingly as the origin is approached. We can include an infinite number of eigenmodes making ν imaginary, but for ν imaginary all of these infinite seqüence of imaginary ν_n acumulate at the origin, so we can replace all of these by the singular contribution given by $\nu = 0$[4]. For this reason we represent the non-oscillating modes by a single parabolic cylinder function.

Coming back to the eigenvalue condition, we see that in the first method non-oscillating modes do not introduce contributions for eigenvalues, so we can ignore them, while for last methods this contribution can be relevant.

5 Mean cumulative density of states

The cumulative density of states is important to analyse numerical results. By calculating the deviation relative to the mean cumulative density we have a test for eigenvalue completeness.

We are considering a smooth system, so we can calculate the mean cumulative density of states as [17]:

$$\mathcal{N}(E) = \frac{1}{(2\pi)^2} \int dpdq\ \Theta\left(E - \mathcal{H}(pq)\right). \tag{26}$$

Considering a Hamiltonian given by (1), it will be easy to calculate (26) considering separated partial regions I and II as in the previous section. Starting with region I , a simple transformation $(p_i, q_i) \rightarrow (r_i, \phi_i)$ leads to :

$$\mathcal{N}_1(E) = \frac{1}{4\pi^2} \int_{-\pi/2}^{\pi/2} d\phi_1 \int_{-\pi/2}^{\pi/2} d\phi_2 \int_0^{\kappa} dr_1 r_1 \int_0^{\sqrt{\kappa^2 - r_1^2}} dr_2 r_2 = E^2/8 \ \ ; \kappa^2 = 2E\,. \tag{27}$$

Considering region II, a similar transformation $(p_y, y) \rightarrow (r, \phi)$ leads to

$$\mathcal{N}_2(E) = \frac{1}{4\pi^2} \int_{-b}^{0} dx \int_0^{\kappa} dp_y \int_{-\pi/2}^{\pi/2} d\phi_2 \int_0^{\sqrt{\kappa^2 - p_y^2}} dr_2 r_2 = \frac{\sqrt{2}}{3\pi} b \sqrt[3]{E} \ \ ; \kappa^2 = 2E\,. \tag{28}$$

Finally adding (27) and (28) we obtain

$$\mathcal{N}(E) = \frac{1}{8}E^2 + \frac{\sqrt{2}}{3\pi}b\sqrt[3]{E}\ . \tag{29}$$

6 Results and discussions

The methods developed in last sections are very efficient. Calculating eigenvalues using the first method we just have to evaluate the wronskian of the transversal eigenmodes, while for the second method and its asymptotic approximation we need to evaluate the determinant of matrices whose dimensions are given by the integer part of the real quantity $\left(\frac{1}{2}\left[E+1\right]+1\right)$, including evanescent modes.

Testing eigenvalue completness, figure 3.a shows the cumulative density of states and figure 3.b shows the deviation relative to the mean cumulative denstity of states; full lines in figure 3.a are obtained using (29). It is important to point that, in our theory, the role of non-oscillating modes is to improve eigenvalues. In fact the first method does not need non-oscillating modes , because of this reason this method is exact and it will become useful as a pattern.

Figure 4.a shows the relative deviation between eigenvalues obtained using the second method and the first method, while figure 4.b shows the relative deviation for eigenvalues obtained using the asymptotic method and the first method , respectively. For both of them, we have expressed the relative deviation in units of the mean level spacing. Figure 5 shows the nearest neighbour density of eigenvalues that is compared with the Poisson distribution.

By showing the excelent agreement between eigenvalues using the quantum section method and the ones obtained using the exact method, our goal is to show numerical feasibility for the former. Although our realization treated with an integrable problem when $\alpha = 1$, the asymptotic method developed in section 3 is easily generalized for the cases $\alpha > 1$, and it will provide a good tool to enlighten this important system in its mixed regime. The only change in the general case will occur in the detailed form of the one dimensional solutions (20) and (24), where we must relie on numerical integration of the actions. A point of paramount importance here is that there is no exact solution for this general problem. Work is in progress in this direction.

Acknowledgements

We thank Dr. R. Vallejos for valuable discussions. JSEO. specially acknowledge support from FAPERJ (Fundação de Amparo à Pesquisa do Estado de Rio de Janeiro), contract number $E-26/\ 150.155\ /97$.

Appendix

A Developing W.K.B. theory for radial functions

Following W.K.B. theory applied to two turning points, we calculate the radial function starting from the region on the left of r_1:

$$\zeta(r)\begin{cases} \frac{1}{\sqrt[4]{\frac{\nu^2}{r^2}+r^2-\kappa^2}}\exp \mathrm{s}_<(r) & ;\, 0<r<r_1\,, \\ \frac{2}{\sqrt[4]{\kappa^2-\frac{\nu^2}{r^2}-r^2}}\cos\left(\mathrm{s}(r)-\frac{\pi}{4}\right) & ;\, r_1<r<r_2\,, \end{cases} \tag{30}$$

where

$$\begin{aligned} \mathrm{s}_<(r) &= \int_r^{r_1} dr\sqrt{\tfrac{\nu^2}{r^2}+r^2-\kappa^2}\,; \\ &= \tfrac{1}{2}\sqrt{\nu^2+r^4-\kappa^2 r^2}-\log\left\{\left(\frac{\frac{2\nu^2}{r^2}+\frac{2\nu}{r}\sqrt{\frac{\nu^2}{r^2}+r^2-\kappa^2}-\kappa^2}{\sqrt{\kappa^2-4\nu^2}}\right)^{\nu/2}\left(\frac{2r^2+2\sqrt{\nu^2+r^4-\kappa^2r^2}-\kappa^2}{\sqrt{\kappa^4-4\nu^2}}\right)^{\kappa^2/4}\right\}, \end{aligned} \tag{31}$$

$$\mathrm{s}(r) = \int_{r_1}^{r} dr\sqrt{\kappa^2-\tfrac{\nu^2}{r^2}-r^2}\,. \tag{32}$$

Looking for solutions on the right of the turning point (r_2), we decompose the action, between the two turnig points, in the following form

$$\begin{aligned} \cos\left(\mathrm{s}(y)-\tfrac{\pi}{4}\right) &= \cos\left(\textstyle\int_{r_1}^{r}[\cdot]dy-\frac{\pi}{4}\right); \\ &= \cos\left(\textstyle\int_{r_1}^{r_2}[\cdot]dy-(\mathrm{s}_{1,2}(r)-\frac{\pi}{4})-\frac{\pi}{2}\right); \\ &= \sin\left(\textstyle\int_{r_1}^{r_2}[\cdot]dy-(\mathrm{s}_{1,2}(r)-\frac{\pi}{4})\right); \\ &= \sin\left(\textstyle\int_{r_1}^{r_2}[\cdot]dr\right)\cos\left(\mathrm{s}_{1,2}(r)\right)-\cos\left(\textstyle\int_{r_1}^{r_2}[\cdot]dr\right)\cos\left(\mathrm{s}_{1,2}(r)\right), \end{aligned} \tag{33}$$

where $[.]=\sqrt{\kappa^2-\frac{\nu^2}{r^2}-r^2}$. Only the first term on the right of (33) will let the function on the right of r_2 become decresing when $r\to\infty$[12]. For this reason we impose that

$$\cos\left(\int_{r_1}^{r_2} dr\sqrt{\kappa^2-\frac{\nu^2}{r^2}-r^2}\right)=0\,, \tag{34}$$

and from here

$$\int_{r_1}^{r_2} dr\sqrt{\kappa^2-\frac{\nu^2}{r^2}-r^2}=(2m-1)\,\frac{\pi}{2}\,;\;\; m\geq 1. \tag{35}$$

Because of this matching condition we can write the radial function , excluding turning points, by:

$$\psi_1=\begin{cases} \frac{2/\sqrt{r}}{\sqrt[4]{\frac{\nu^2}{\kappa^2}+r^2-\kappa^2}}\exp \mathrm{s}_<(r) & ;r<r_1\,, \\ (-1)^{m+1}\,\frac{2/\sqrt{r}}{\sqrt[4]{\kappa^2-\frac{\nu^2}{\kappa^2}-r^2}}\cos\left(\mathrm{s}_{1,2}(r)-\frac{\pi}{4}\right) & ;r_1<r<r_2\,, \\ \frac{2/\sqrt{r}}{\sqrt[4]{\frac{\nu^2}{\kappa^2}+r^2-\kappa^2}}\exp -\mathrm{s}_>(r) & ;r>r_2\,, \end{cases} \tag{36}$$

where actions are given by the expressions[18]

$$\begin{aligned} \mathrm{s}_{>}(r) &= \int_{r_2}^{r} dr \sqrt{\tfrac{\nu^2}{r^2} + r^2 - \kappa^2} \; ; \\ &= \tfrac{1}{2}\sqrt{\nu^2 + r^4 - \kappa^2 r^2} - \log \left\{ \left(\frac{\kappa^2 - \frac{2\nu^2}{r^2} - \frac{2\nu}{r}\sqrt{\frac{\nu^2}{r^2} + r^2 + \kappa^2}}{\sqrt{\kappa^2 - 4\nu^2}} \right)^{\nu/2} \left(\frac{2r^2 + 2\sqrt{\nu^2 + r^4 - \kappa^2 r^2} - \kappa^2}{\sqrt{\kappa^4 - 4\nu^2}} \right)^{\kappa^2/4} \right\} \end{aligned} \tag{37}$$

and

$$\begin{aligned} \mathrm{s}_{1,2}(r) &= \int_{r}^{r_2} dr \sqrt{\kappa^2 - \tfrac{\nu^2}{r^2} - r^2} \; ; \\ &= \left(\tfrac{\kappa^2}{2} - \nu \right) \tfrac{\pi}{4} - \tfrac{r}{2}\sqrt{\kappa^2 - \tfrac{\nu^2}{r^2} - r^2} + \tfrac{\nu}{2} \arcsin \tfrac{\kappa^2 - \frac{2\nu^2}{r^2}}{\sqrt{\kappa^4 - 4\nu^2}} + \tfrac{\kappa^2}{4} \arcsin \tfrac{\kappa^2 - 2r^2}{\sqrt{\kappa^4 - 4\nu^2}} \, . \end{aligned} \tag{38}$$

From (35) we find the quantization condition of angular momenta, ie:

$$s_{1,2}(r_1) = (2m - 1)\tfrac{\pi}{2} \, , \tag{39}$$

where

$$\nu = (E + 1 - 2m) \; ; \quad m \geq 1 \, . \tag{40}$$

List of figures

Figure 1: The soft stadium. The concentric lines are described by equipotentials with outer lines of higher energy than the inner ones. The Poincaré section Σ is defined by the vertical dotted line, and it separates region I and II.

Figure 2: In figure 2.a, a classical periodic orbit in the configuration space with $t_x = \pi$. In figure 2.b , the Poincaré map obtained with 500 iterations for a trajectory with $t_x = \pi + 0.1$.

Figure 3: The cumulative density of states (step) and the mean cumulative density of states (continuous line) are showed in figure 3.a . The deviation relative to the mean cumulative density of states is showed in figure 3.b .

Figure 4: Relative deviation between eigenvalues in units of the mean level spacing . In figure 4.a we compared the first two methods, while in figure 4.b we compare the assymptotic approximation and the first method .

Figure 5: The nearest neighbour density for eigenvalues. The continuous line represents the Poisson distribution.

References

[1] Bogomolny E, 1990 Comments Atomic Molecular Phys 25 67.

[2] Bogomolny E, 1992 Nonlinearity 5 805

[3] Ozorio de Almeida AM, J Phys A: Math. Gen 27 (1994) 2891-2904

[4] J. S. Espinoza Ortiz and A. M. Ozorio de Almeida, J.Phys. A:Math Gen,30 (1997) 7301-7313.

[5] E. Doron and U. Smilansky, Nonlinearity 5 (1992) 10055.

[6] P.A. Boasman, Nonlinearity 7 (1994) 485.

[7] E. Vergini and M. Saraceno, Phys Rev E52 (1995) 2204.

[8] H. U. Baranger, R. A. Jalabert, and A.D. Stone, chaos 3:665(1993)

[9] K. Nakamura and H. Ishio , Jour Phys. Soc. Jpn. 61:3939 (1992)

[10] H. Ishio and J. Burgdörfer, Phys. Rev. B 51:2013(1995)

[11] Lichtenbergm A.J. and Lieberman, M.A. (1983). Regular and Irregular Motion. New York: Springer.

[12] P.M. Morse and H. Feshbach, Methods of Theoretical Physics New York : Mc Graw Hill 1953.

[13] M. Abramowitz and A. Stegun, Handbook of Mathematical Functions (New York:Dover 1964)

[14] Eugen Merzbachher,(1970) Quantum Mechanics (John Willey and Sons,Inc).

[15] M. V. Berry and A.M. Ozorio de Almeida, J Phy A:Math, Nucl.Gen Vol 6 (1973).

[16] M.V.Berry and K.E.Mount,(1972) Rep. Progr. Phys. 35,315.

[17] Alfredo M. Ozorio de Almeida, (1988) Hamiltonian Systems: Chaos and Quantization (Cambridge nonographs in mathematical physics).

[18] I.J.Gradshteyn,I.M.Ryzhik, Tables of integrals, series and products,(Academic Press,New York,1980).

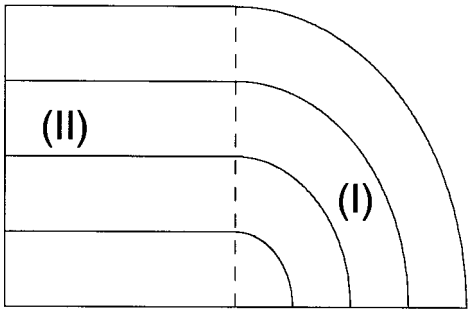

figure 1

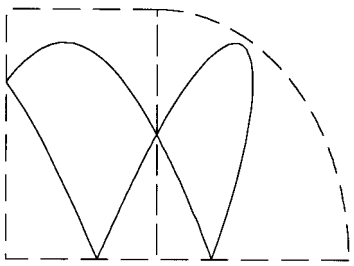

figure 2.a

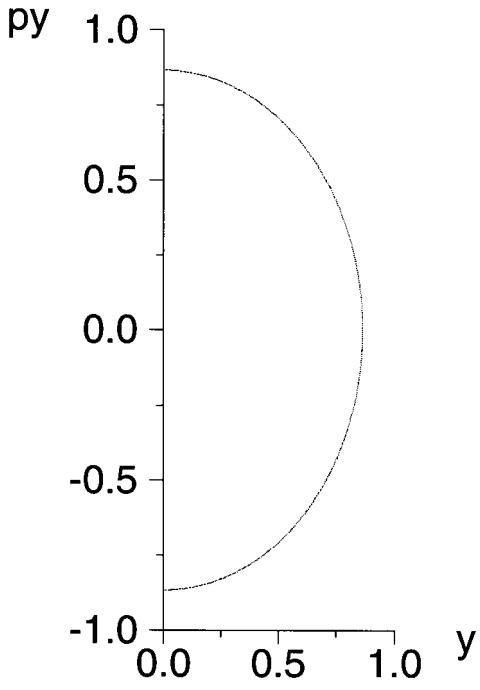

figure 2.b

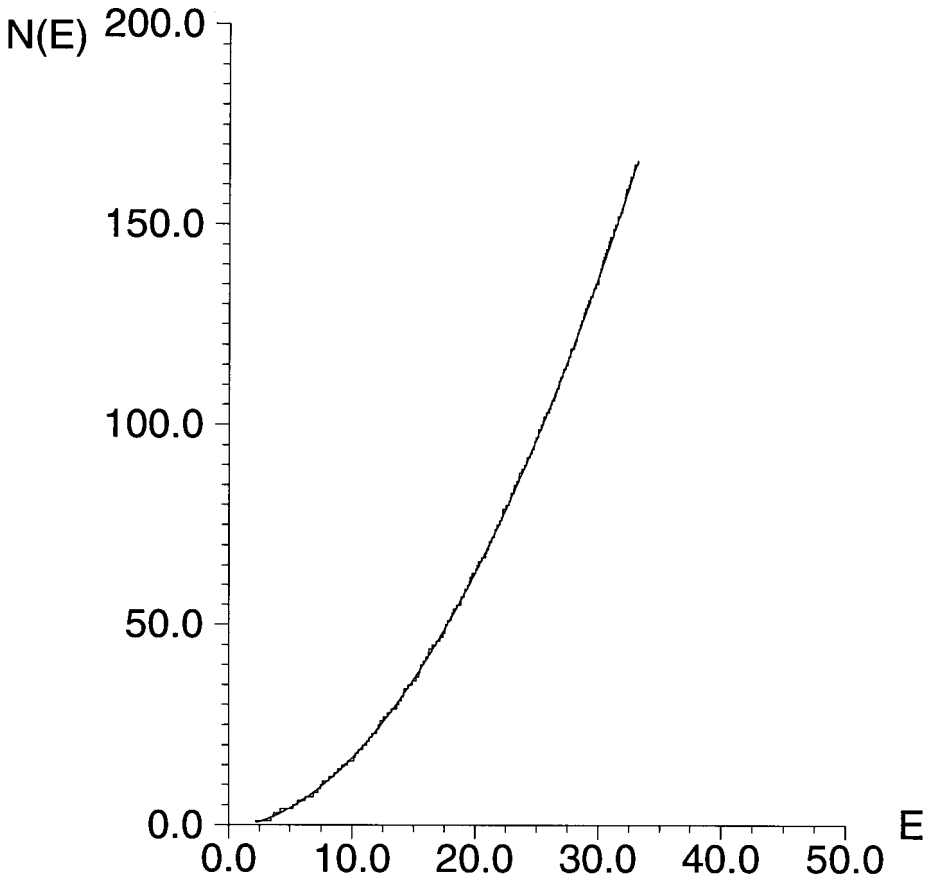

figure 3.a

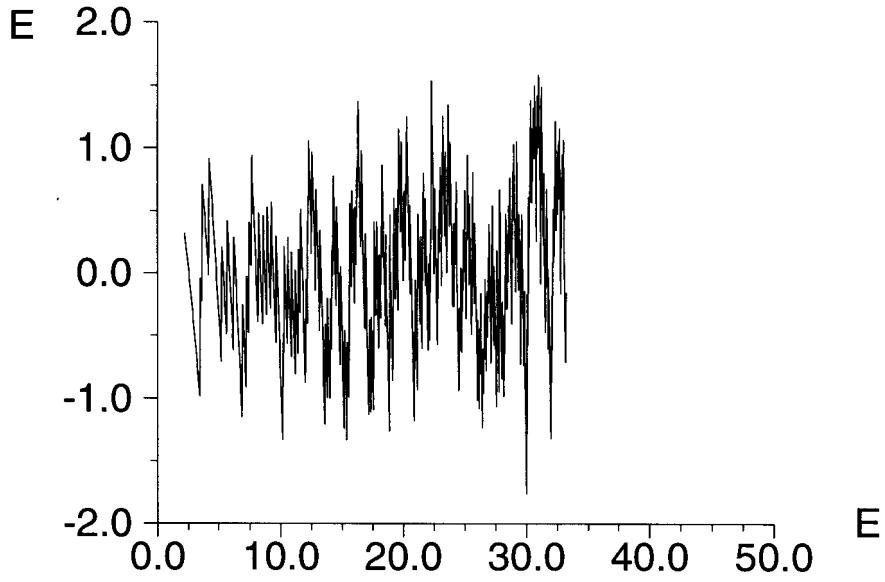

figure 3.b

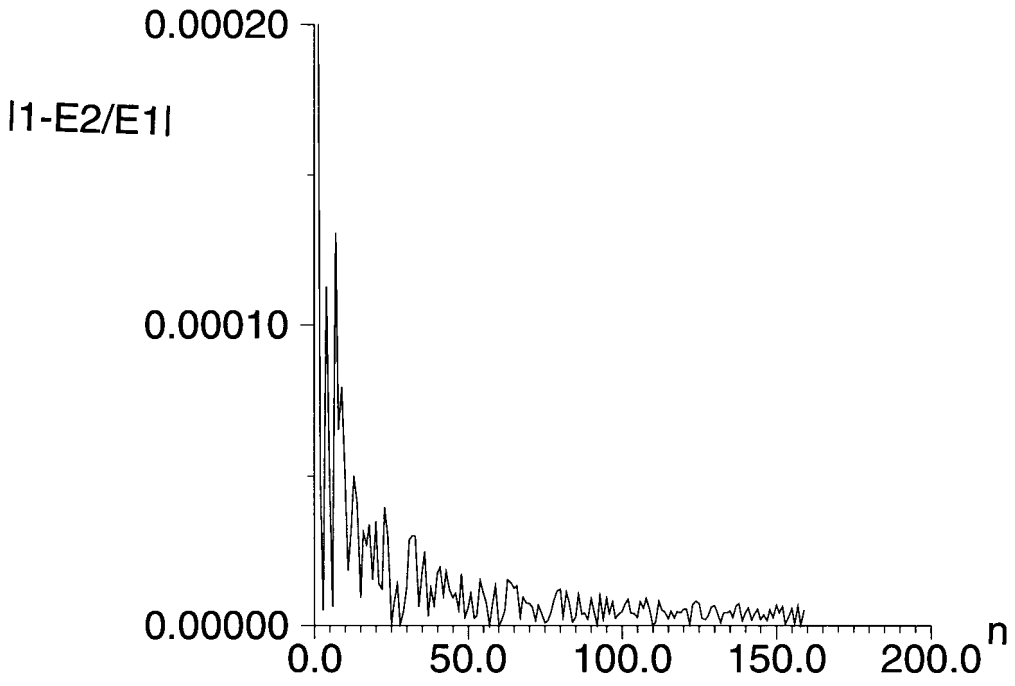

figure 4.a

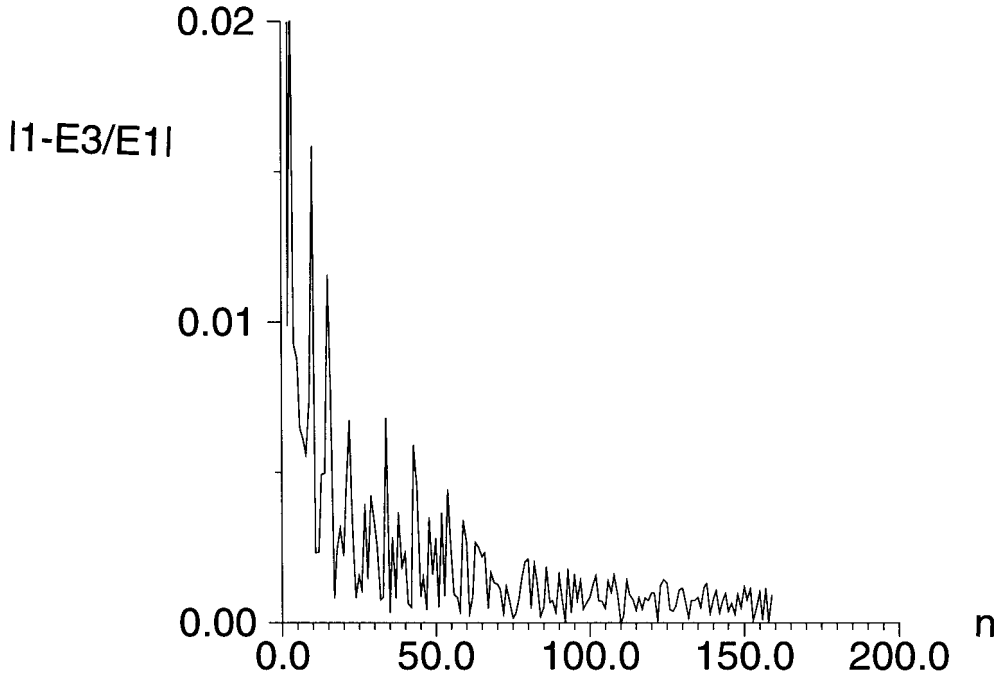

figure 4.b

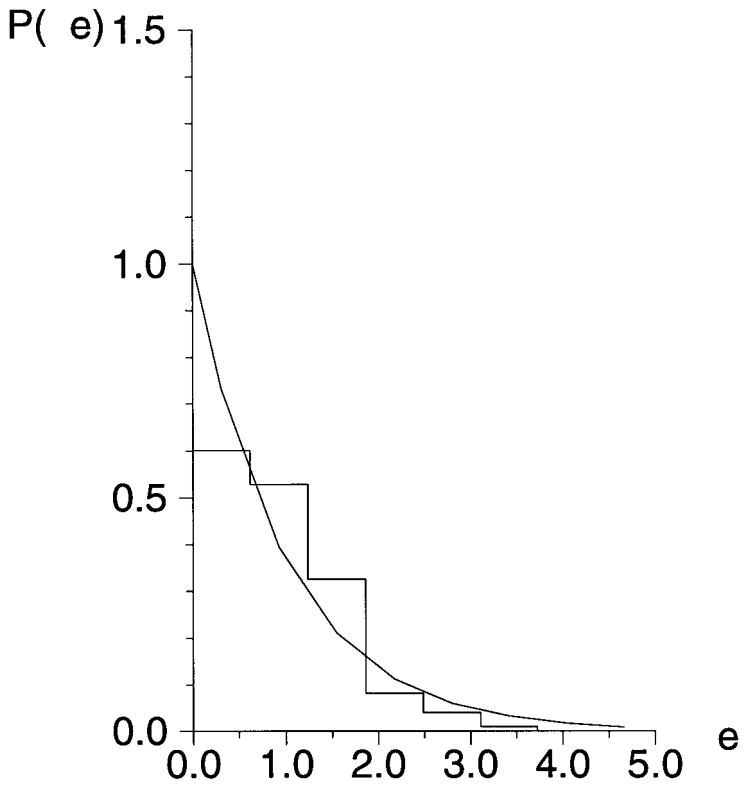

figure 5